International Journal of Chemical and Biochemical Sciences
(ISSN 2226-9614)

Journal Home page: www.iscientific.org/Journal.html

Anti-lung cancer potential of the ethanolic rhizome extract of *Irish versicolor* - A study combining of metabolomic profiling and molecular docking approach

Puja Ghosh[1], Duraiswamy Basavan[2], Antony Justin[1]*

[1]Department of Pharmacology, JSS College of Pharmacy, JSS Academy of Higher Education & Research, Ooty, Nilgiris, Tamil Nadu , India 643 001

[2]Department of Pharmacognosy, JSS College of Pharmacy, JSS Academy of Higher Education & Research, Ooty, Nilgiris, Tamil Nadu , India 643 001

Abstract

Intrinsic resistance may also be brought about by concurrent molecular or genetic alterations that may diminish the susceptibility of individuals with sensitising EGFR mutations to EGFR-TKI treatment. EGFR-TKI plays a crucial modulator role in cell growth, cell survival and in case of induction of apoptosis in non-small cell lung cancer with EGFR mutation. The goal of this work is to present a bioactive phytoconstituents that inhibit the EGFR-TKI domain what would be effective in cancer treatment with producing minimal side effects. We have selected the *Iris versicolor* (Iridaceae) plant, which is used to treat cancer and is regarded as one of the powerful traditional treatments in the Indian Ayurvedic medicinal system. Through the use of the HR-LCMS Assisted phytochemical screening approach, we have conducted an exploration and reported the bioactive phytoconstituents found in the rhizome of the Iris versicolor plant in a scientific manner. Molecular docking study has performed using Schrödinger's toolkit to anticipate the binding affinities and modes of compound Trihydroxycholestanoic acid and its interactions with EGFR. The examination of protein-ligand contacts revealed that the compound's favourable binding affinity is mostly due to large hydrophobic contacts, stabilising salt bridges, and strong hydrogen bonding interactions.

Keywords: *Iris versicolor*, EGFR-TKI, Molecular docking, Trihydroxycholestanoic acid, MDR NSCLC

Full length article **Corresponding Author*, e-mail: justin@jssuni.edu.in

1. Introduction

One of the leading causes of death in the globe is cancer. Chemotherapy is still the most often used cancer treatment, even after several decades. One of the main causes of chemotherapy failure in cancer patients is the development of multidrug resistance in cancer cells [1]. The ability of cancer cells to develop resistance to anti-cancer drugs that are structurally and functionally unrelated is referred to as "multidrug resistance". One of the primary problems with cancer treatment is the emergence of multidrug resistance (MDR) to chemotherapy [2]. Multidrug resistance (MDR) is caused by a number of factors, including growth regulators, enhanced drug uptake, maximal drug efflux, detoxification systems, increased xenobiotic metabolism, accelerated DNA repair potential, preventing drug-induced apoptosis, and genetic factors like gene mutations, epigenetic modifications, and amplifications. Consequently, transport proteins play a crucial role in the development of multidrug resistance (MDR); they accomplish this by effluxing chemotherapeutic drugs from cells and inhibiting the intracellular accumulation of the treatments [3]. A growing number of biomedical research studies are focusing on developing chemotherapeutics that can prevent or reverse this mechanism due to the rising death rate, which is attributed to the MDR in 90% of cancer patients receiving chemotherapeutic treatment [4]. A thorough understanding of the procedures that could be used to prevent and treat drug resistance. Globally, lung cancer has the highest rates of both morbidity and mortality. 2018 had a total of 18.1 million new cases in both sexes and 9.6 million deaths from cancer reported. This is a status report on the worldwide cancer burden, per the GLOBOCAN 2018 report from the International Agency for Research on Cancer [5].

According to estimates, lung cancer claimed the lives of 1.8 million people in 2018, making up around 25% of all cancer-related deaths [5]. Histology indicates that around

85% of cases of lung cancer are advanced stage non-small-cell lung cancer (NSCLC) [6]. Because at the time of diagnosis, more than half of individuals with newly diagnosed NSCLC already had advanced disease. The median overall survival (OS) is fewer than 12 months despite advancements in treatment [7]. For activated genetic mutations or fusions in the epidermal growth factor receptor (EGFR; also known as ERBB1), anaplastic lymphoma kinase (ALK), ROS1 proto-oncogene receptor tyrosine kinase (ROS1), and serine/threonine-protein kinase b-raf (BRAF) in NSCLC, tyrosine-kinase-inhibitor therapy has emerged as the main targeted therapy [8-10]. The therapy and drugs used to treat lung cancer have long-term negative effects as well as drug-related side effects. Because of this, the available treatment is not optimal [11]. Because they are widely available in India and can treat cancer without having any unfavourable side effects, we are focusing on the historically used medicinal herbs instead of synthesised drugs. The Iridaceae is a vast family of rhizome- or corm-bearing perennial herbaceous plants that includes 82 genera and around 1750 species. This family of plants can be found in both temperate and tropical regions of the world; South Africa has the most diversity, followed by South America, Europe, and the temperate portions of Asia [11]. Even though the constituents of iris species have been found to possess a variety of activities, including antiulcer, antibacterial, anti-inflammatory, antineoplastic, antioxidant, and hypolipidemic properties, they have been used extensively in traditional medicine to treat cancer, inflammation, and viral and bacterial infections.

2. Materials and Methods

2.1. Collection and preparation of medicinal plant extract

The rhizome of the *Iris versicolor* plant has been taken from the Kashmir University botanical garden and the surrounding graveyard area. Dr. Anzar Khuroo, the taxonomist from Kashmir University's Department of Taxonomy, has verified the authenticity of the plant. 100 grammes of dried plant rhizome were utilised to create an ethanolic extract using the soxhlet equipment, and extracts were made using the three times ethanolic extraction procedure. Subsequent extracts were kept at 4°C and concentrated using a rotary evaporator set at 40°C.

2.2. HR-LCMS analysis for the Identification of Bioactive Compounds

An Agilent 324 Technologies®, USA, system including the HR-LCMS 1290 Infinity stands for UHPLC System Ultra High-performance Liquid Chromatography Photodiode-Array Detector 323 Mass Spectrophotometer was used to analyse the phytochemistry of Iris versicolor rhizome. A dual Agilent Jet Stream Electrospray (AJS ES) ion source, quadrupole Time of Flight Mass Spectrometer (MS Q-TOF), column compartment, and HiP sampler were the parts of the liquid chromatographic system. 10 µL of sample was added to the apparatus, and separation was carried out using the SB-C18 column (2.1 × 50 mm, 1.8 µm particle size). Acetonitrile (solvent B) and 1% formic acid in deionized water (solvent A) were the solvents used. For MS detection, a flow rate of 0.350 mL/min was utilised in conjunction with MS Q-TOF. Compounds were identified by their unique mass fragmentation patterns and mass spectra. To identify the phytochemical constituents, the main resources used were Compound Discoverer 2.1, PubChem, and ChemSpider.

2.3. Insilico-molecular docking study

To evaluate our rhizome extract's inhibitory potential on the epidermal growth factor receptor (EGFR), we employed a multistep methodology. First, we improved our knowledge of the 3D architecture of EGFR by gathering structural insights from the Protein Data Bank (PDB) at https://www.rcsb.org/. Subsequently, we performed molecular docking experiments using Schrodinger's suite of tools available at https://www.schrodinger.com/products/maestro to forecast potential interactions between EGFR and the 86 components of our plant extract. This phase allowed us to look at binding affinities and modes to predict possible inhibitory effects. We next conducted ADMET (Absorption, Distribution, Metabolism, Excretion, and Toxicity) tests to assess the components' pharmacokinetic characteristics.

2.4. Ligand preparation of all rhizome Extract Constituents

To synthesize ligands from the components of the rhizome extract, we utilised the Ligprep interface found in the Schrödinger software package (version 2021-4, maestro 12.6). This important step was to convert the inhibitors' 2D structures into 3D structures that could be subjected to rigorous computational analysis. Several crucial processes, including as hydrogen addition, conformational optimisation, and bond order assignment, were made easier by the Ligprep tool. These procedures were essential to guarantee that the ligands were formatted correctly for the ensuing computer analysis. Ligprep produced a spectrum of protonation and ionisation states under varied pH settings, accounting for tautomeric and ionisation forms as well. It also investigated other tautomeric structures, broadening the range of ligand conformations that our study considered. We methodically produced the ligands obtained from the elements of the rhizome extract by using Ligprep, which laid the foundation for accurate and thorough analysis in the latter phases of our investigation.

2.5. Selection of Epidermal Growth Factor Receptor (EGFR) Protein from Protein Data Bank

The 1M14 PDB ID, which represents the Tyrosine Kinase Domain of the Epidermal Growth Factor Receptor (EGFR), was the deliberate focus of our investigation. The pivotal function of EGFR in the advancement of cancer serves as the basis for this decision. The chosen protein, which comes from humans and was identified at 2.60 Å resolution by X-RAY DIFFRACTION, captures a detailed knowledge of the structural details of EGFR. Interestingly, the crystal structure offers a comprehensive view of the EGFR Tyrosine Kinase Domain, containing forty amino acids from the carboxyl-terminal tail. The EGFR Tyrosine Kinase Domain is not normally phosphorylated, but it does have a conformation that is like the phosphorylated active form of other receptor tyrosine kinases.

Figuring out the molecular processes behind the development and spread of cancer requires an understanding of the structural subtleties of EGFR, particularly its kinase domain. Our work, which focuses on the 1M14 PDB ID, is in line with the larger objective of using this information to create targeted therapies that could interfere with EGFR-

related signalling pathways linked to several cancers. This could open the door to more efficient and individualised cancer treatments [12].

2.6. Preparation of EGFR Receptor (PDB ID: 1M14) for Cancer Treatment

We concentrated on the Tyrosine Kinase Domain, which is important for cancer pathways, to get our EGFR receptor (PDB ID: 1M14) ready for therapy investigation. Using the Schrödinger software suite 2021–24's Maestro interface, we painstakingly created a three-dimensional structure by eliminating unnecessary water molecules and distracting ligands. This preparation preserves the structural integrity of EGFR, which is in line with our goal of treating cancer. The selected 1M14 structure provides a basis for investigating inhibitory mechanisms, and a Ramachandran plot analysis was used to confirm its dependability, making it suitable for reliable computer simulations. This thorough preparation creates a strong foundation for identifying complex relationships and possible inhibitory effects that are essential for creating targeted treatments against cancer's EGFR-related signaling pathways [13-14].

2.7. Molecular docking using Glide

With the components of our rhizome extract and the active site (1M14) of the EGFR protein, we used Schrödinger's Maestro programme 2021-24 and its potent tool, Glide, for molecular docking. With ligand sampling set to "none refine only" in XP mode for exact precision, Glide enabled us to investigate how our rhizome extract constituents fit tightly into EGFR's critical area. Not only did this docking research solve puzzles, but it also provided important information about the ligands' binding affinities and possible interactions with EGFR. The ability to visualize these interactions was facilitated by the ligand interaction tool, which provided a clear image of the hydrophobic and hydrogen bond interactions between the ligands and certain amino acids in the protein.

3. Results

3 Metabolomic profiling.1.

We performed a high resolution-liquid chromatography-mass spectrometry analysis (HR)-LCMS on the ethanolic extract of *Iris versicolor* rhizome. As shown in Table 1 and in chromatogram (Figure 1), the results showed the presence of 56 compounds, of which 32 main compounds were confirmed based on their retention time, mass, and molecular formula. The chromatogram shows the relative concentrations of the several compounds that eluted as a function of retention time. The height of the peak indicates the relative quantities of bioactive substances. Using a mass spectrometer, the structure of unknown compounds that are eluted at different times is investigated. We effectively collected and processed every component from the rhizome extract in our extensive investigation, and we also painstakingly confirmed the structural integrity of our target protein, EGFR.

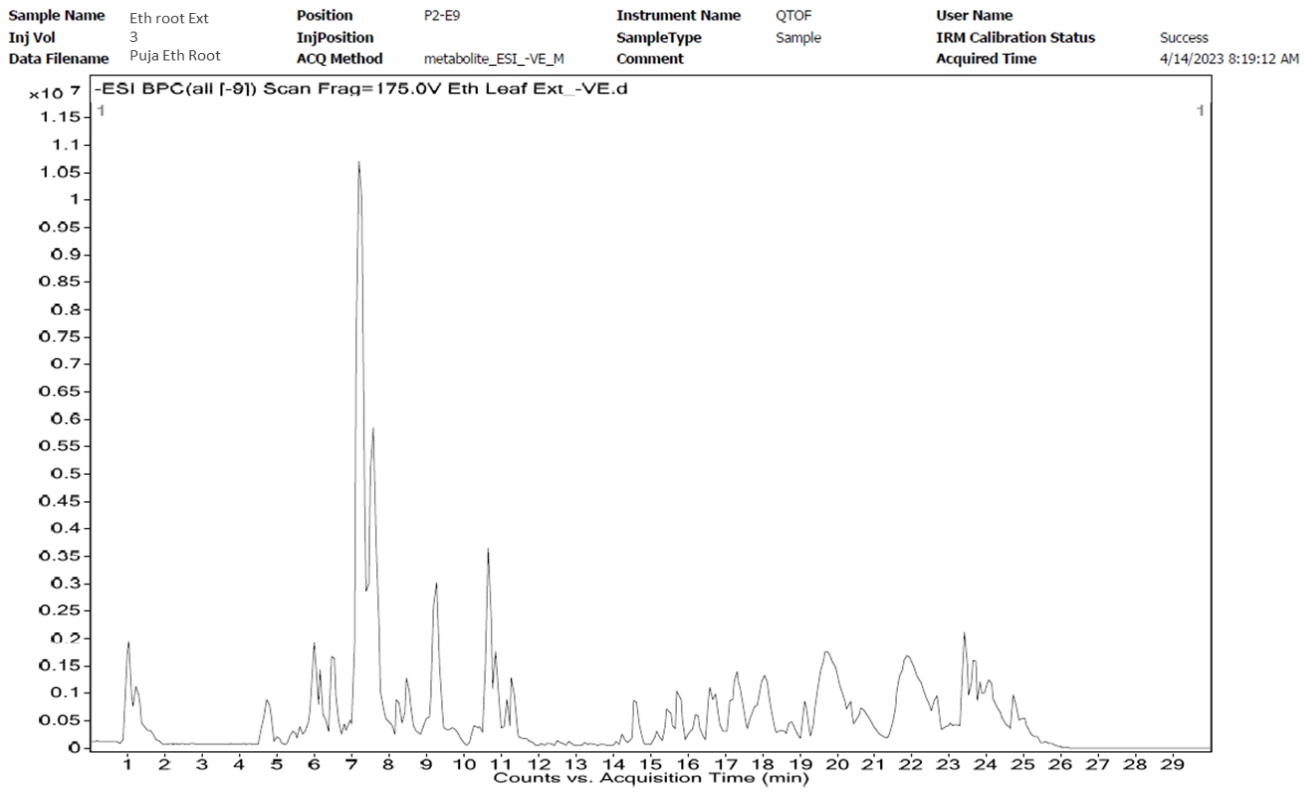

Figure 1: HR-LCMS Spectrogram of ethanolic extract of Iris versicolor leaves.

Table 1: Bioactive phytoconstituents in ethanolic extract of Iris versicolor leaves.

SL No	Name	Formula	Score	Mass	Mass (DB)
1	Feruloyl-2-hydroxyputrescine	$C_{14}H_{20}N_2O_4$	60.03	280.1375	280.1423
2	Methylarbutin	$C_{13}H_{18}O_7$	77.96	286.1026	286.1053
3	Fortimicin A	$C_{17}H_{35}N_5O_6$	93.55	405.2595	405.2587
4	Methylarbutin	$C_{13}H_{18}O_7$	80.25	286.1027	286.1053
5	Hispidulin	$C_{16}H_{12}O_6$	58.33	300.0583	300.0634
6	O-Demethylfonsecin	$C_{14}H_{12}O_6$	66.08	276.0609	276.0634
7	Glycylprolylhydroxyproline	$C_{12}H_{19}N_3O_5$	88.67	285.1321	285.1325
8	5,6:8,9-Diepoxyergost-22-ene-3,7beta-diol	$C_{28}H_{44}O_4$	57.18	444.3205	444.324
9	Teasterone	$C_{28}H_{48}O_4$	57.64	448.3538	448.3553
10	5,6-Epoxiergosta-8,22-diene-3,7-diol	$C_{28}H_{44}O_3$	44.96	428.3237	428.329
11	3,5,9-Trihydroxyergost-7-en-6-one	$C_{28}H_{46}O_4$	48.23	446.3349	446.3396
12	23-Acetoxysoladulcidine	$C_{29}H_{47}NO_4$	64.73	473.3467	473.3505
13	20-Hydroxycholesterol	$C_{27}H_{46}O_2$	77.62	402.3465	402.3498
14	Ganodermic acid Jb	$C_{30}H_{46}O_4$	14.58	466.3071	470.3396
15	1-Monopalmitin	$C_{19}H_{38}O_4$	72.4	330.2745	330.277
16	alpha-Micropteroxanthin B	$C_{27}H_{40}O_2$	68.6	396.2995	396.3028
17	Coprocholic acid	$C_{27}H_{46}O_5$	70.2	450.3304	450.3345
18	22,23-Dihydroergosterol	$C_{28}H_{46}O$	70.4	398.3509	398.3549
19	5-(12,15-Heneicosadienyl)-1,3-benzenediol	$C_{27}H_{44}O_2$	68.3	400.3306	400.3341
20	Methyl 2-(10-heptadecenyl)-6-hydroxybenzoate	$C_{25}H_{40}O_3$	75.98	388.2943	388.2977
21	7-Oxatyphasterol	$C_{28}H_{48}O_5$	68.29	464.3455	464.3502
22	(3beta,4alpha,5alpha)-4-Methyl-8(14)-cholesten-3-ol	$C_{28}H_{48}O$	70.27	400.3664	400.3705
23	N-Nitrosotomatidine	$C_{27}H_{44}N_2O_3$	47.18	444.3356	444.3352
24	Betulin	$C_{30}H_{50}O_2$	57.26	442.3747	442.3811
25	Esculetin	$C_9H_6O_4$	69.88	178.026	178.0266
26	ent-Epicatechin-(4alpha->8)-ent-epicatechin 3'-gallate	$C_{37}H_{30}O_{16}$	64.44	730.1547	730.1534
27	Spinosin C	$C_{37}H_{38}O_{17}$	56.07	754.2014	754.2109
28	Heme C	$C_{40}H_{46}FeN_6O_8S_2$	23.46	856.2103	856.2215
29	Phytosulfokine a	$C_{33}H_{46}N_6O_{16}S_2$	48.03	846.2499	846.2412
30	Vitisifuran B	$C_{56}H_{40}O_{12}$	81.09	904.2545	904.252
31	Myricetin 3-[glucosyl-(1->2)-rhamnoside] 7-[rhamnosyl-(1->2)-glucoside]	$C_{39}H_{50}O_{26}$	72.7	934.2654	934.259
32	Carthamin	$C_{43}H_{42}O_{22}$	64.17	910.2189	910.2168
33	Aflatoxin B1 dialdehyde	$C_{17}H_{14}O_8$	56.96	346.0631	346.0689
34	1,2,2'-Trisinapoylgentiobioside	$C_{45}H_{52}O_{23}$	62.52	960.2809	960.2899
35	4',5,7-Trihydroxy-3-methoxyflavanone	$C_{16}H_{14}O_6$	55.75	302.0731	302.079
36	3,4,3'-Tri-O-methylellagic acid	$C_{17}H_{12}O_8$	58.53	344.0476	344.0532
37	Aflatoxin GM1	$C_{17}H_{12}O_8$	56.67	344.0472	344.0532
38	Capsianoside III	$C_{50}H_{84}O_{26}$	74.69	1100.5319	1100.5251
39	Gingerglycolipid A	$C_{33}H_{56}O_{14}$	60.71	676.3598	676.367
40	Gingerglycolipid B	$C_{33}H_{58}O_{14}$	7.75	678.3748	678.3827
41	Flavidulol C	$C_{34}H_{42}O_4$	88.33	514.3075	514.3083
42	Gallopamil	$C_{28}H_{40}N_2O_5$	47.92	484.2985	484.2937
43	3alpha,7alpha-Dihydroxy-12-oxo-5beta-cholan-24-oic Acid	$C_{24}H_{38}O_5$	27.31	406.2799	406.2719
44	Isoglabrolide	$C_{30}H_{44}O_4$	58.98	468.3176	468.324
45	Mucronine A	$C_{29}H_{38}N_4O_4$	43.74	506.2929	506.2893
46	Actinidic acid	$C_{30}H_{46}O_5$	57.46	486.3279	486.3345
47	LysoPE(20:2(11Z,14Z)/0:0)	$C_{25}H_{48}NO_7P$	39.51	505.3076	505.3168
48	Thermozeaxanthin-13	$C_{59}H_{90}O_8$	71.42	926.6568	926.6636
49	Aromoline	$C_{36}H_{38}N_2O_6$	70.91	594.2739	594.273
50	Guattegaumerine	$C_{36}H_{40}N_2O_6$	77.93	596.2905	596.2886
51	Daphnandrine	$C_{36}H_{38}N_2O_6$	67.41	594.2739	594.273
52	Ethyl 2E,4Z-hexadecadienoate	$C_{18}H_{32}O_2$	59.23	280.2354	280.2402
53	Elaidolinoleic acid	$C_{18}H_{30}O_2$	40.71	278.2193	278.2246
54	Tributyl phosphate	$C_{12}H_{27}O_4P$	92.5	266.1648	266.1647
55	3-Pentadecylphenol	$C_{21}H_{36}O$	56.45	304.2709	304.2766
56	Stearic acid	$C_{18}H_{36}O_2$	59.76	284.2667	284.2715

Table 2: Docking Results of top 20 rhizome extract constituents with EGFR Protein.

Compound code	Glide Gscore	Glide evdw	Glide ecoul	Glide emodel	Glide energy
Trihydroxycholestanoic acid	-8.49879	-11.712	-29.9718	-80.474	-41.6838
Hispidulin	-8.27592	-28.4709	-20.4171	-79.0098	-48.888
Guattegaumerine	-7.74207	-47.0451	-18.9046	-104.146	-65.9498
O-Demethylfonsecin	-7.14957	-26.5873	-21.4519	-77.4048	-48.0391
Gingerglycolipid A	-6.80293	-39.3491	-30.3821	-94.7599	-69.7312
Aflatoxin GM1	-6.70498	-35.3858	-11.1278	-67.7912	-46.5136
Esculetin	-6.60863	-14.7479	-21.8068	-57.9315	-36.5547
ent-Epicatechin-(4alpha->8)-ent-epicatechin 3'-gallate	-6.52245	-48.4376	-20.7916	-93.5081	-69.2292
Feruloyl-2-hydroxyputrescine	-6.42945	-25.2711	-25.8047	-77.4536	-51.0758
Methylarbutin	-6.26048	-18.3269	-27.4845	-69.8498	-45.8115
3,5,9-Trihydroxyergost-7-en-6-one	-6.28151	-11.112	-20.5113	-37.2864	-31.6233
1617-49-8; 2,3,8-Tri-O-methylellagic acid	-6.06132	-39.1455	-7.9707	-65.7792	-47.1162
Gingerglycolipid B	-6.03718	-37.3007	-20.7537	-74.63	-58.0543
Gallopamil	-5.82115	-44.6845	-11.285	-67.5127	-55.9695
5-(12,15-Heneicosadienyl)-1,3-benzenediol	-5.57716	-37.5887	-22.0368	-78.1434	-59.6255
5,6:8,9-Diepoxyergost-22-ene-3,7-diol	-5.43525	-35.0324	-3.76669	-45.4335	-38.7991
Methyl 2-(10-heptadecenyl)-6-hydroxybenzoate	-5.29748	-22.6632	-44.0916	-64.6232	-66.7548
stearic acid	-4.97158	-25.2367	-22.0338	-71.7633	-47.2704
7-Oxatyphasterol	-4.89299	-28.5872	-14.6045	-52.0433	-43.1917
3-Pentadecylphenol	-4.2344	-30.0746	-9.21527	-44.8217	-39.2899

3.2. Molecular Docking Results for Top 20 Compounds

We performed molecular docking studies to evaluate the inhibitory ability of 86 plant rhizome extract constituents on the EGFR target protein (PDB ID: 1M14) as part of our effort to discover possible cancer treatment options. The molecular docking findings for the top 20 molecules, as determined by different Glide score factors, are shown in Table 2. The overall docking score is represented by the Glide Gscore, where higher binding affinities are indicated by more negative values. Van der Waals and Coulombic interactions between the ligand and the protein are measured by the Glide evdw and ecoul scores, respectively. The Glide energy combines these interactions into a single energy value, and the Glide emodel provides a thorough analysis of the ligand-protein interaction. Compound Trihydroxycholestanoic acid appears to have the greatest binding affinity of any of the top 20 compounds with the EGFR protein, having a severely negative Gscore of -8.49879. This molecule has advantageous van der Waals and Coulombic interactions, with an evdw value of -11.712 and an ecoul value of -29.9718. These factors contribute to an overall favorable Glide energy of -69.5799. Moreover, the emodel score of -80.474 suggests a significant interaction between the chemical and EGFR. These comprehensive molecular docking studies suggest that compound Trihydroxycholestanoic acid is a good candidate for additional study as a potential therapeutic medication targeting EGFR in cancer treatment. The binding affinities and interaction energies of other chemicals in the top 20 list with EGFR also varied. More negative Glide scores and positive interaction patterns indicate that a compound may be an EGFR inhibitor, and it is these compounds that can be chosen for more research, such as ADMET and MM-GBSA tests. Compound Trihydroxycholestanoic acid exhibits robust binding interactions with the EGFR protein.

4. Conclusions

Using (HR)-LCMS high-resolution liquid chromatography-mass spectrometer analysis, the ethanolic extract of rhizome of the *Iris versicolor* plant revealed the presence of bioactive compounds that are therapeutically important. These compounds included flavonoids, glycosides, alkaloids, coumarins, terpenoids, and saponins. These bioactive substances have significant pharmacological properties and may be helpful in the treatment of several human diseases. These bioactive compounds were the subject of additional and *insilico* investigations to find potential therapeutic phytoconstituents for the treatment of cancers.We conducted a thorough investigation into compound Trihydroxycholestanoic acid's potential as an EGFR inhibitor

for cancer treatment during the course of this work. First, we thoroughly evaluated the 3D architecture of EGFR using structural information from the Protein Data Bank (PDB). We performed molecular docking studies using Schrödinger's suite of tools to predict the interaction between compound Trihydroxycholestanoic acid, which is generated from a plant rhizome extract, and EGFR. This phase allowed us to look at binding affinities and modes to predict possible inhibitory effects.

Acknowledgements

The authors enormously acknowledge the Department of Pharmacology, TIFAC- CORE in Herbal Drugs, JSS College of Pharmacy, Ooty for providing infrastructure. Puja Ghosh would like to thank Indian Council of Medical Research (ICMR-SRF 45/17/2022-DDI/BMS) for sanctioned senior research fellowship.

Author Contribution

- **Puja Ghosh:** Conceptualization, Writing-Reviewing.
- **Duraiswamy Basavan:** Visualization, Investigation.
- **Antony Justin:** Supervision, Editing.

Declaration of interest statement

The authors declare that they have no known competing financial interests or personal relationships that could have appeared to influence the work reported in this paper.

References

[1] K. Bukowski, M. Kciuk, R. Kontek. (2020). Mechanisms of Multidrug Resistance in Cancer Chemotherapy. International Journal of Molecular Sciences. 21 (9): 3233.

[2] M. Filipits. (2004). Mechanisms of cancer: Multidrug resistance. Drug Discovery Today: Disease Mechanisms. 1 (2): 229–234.

[3] G. Housman, S. Byler, S. Heerboth, K. Lapinska, M. Longacre, N. Snyder, S. Sarkar. (2014). Drug Resistance in Cancer: An Overview. Cancers. 6 (3): 1769–1792.

[4] X. Wang, H. Zhang, X. Chen. (2019). Drug resistance and combating drug resistance in cancer. Cancer Drug Resistance. 2 (2): 141–160.

[5] F. Bray, J. Ferlay, I. Soerjomataram, R. L. Siegel, L. A. Torre, A. Jemal. (2018). Global cancer statistics 2018: GLOBOCAN estimates of incidence and mortality worldwide for 36 cancers in 185 countries. CA: A Cancer Journal for Clinicians. 68 (6): 394–424.

[6] D. S. Ettinger, D. E. Wood, D. L. Aisner, W. Akerley, J. Bauman, L. R. Chirieac, T. A. D'Amico, M. M. DeCamp, T. J. Dilling, M. Dobelbower, R. C. Doebele, R. Govindan, M. A. Gubens, M. Hennon, L. Horn, R. Komaki, R. P. Lackner, M. Lanuti, T. A. Leal, M. Hughes. (2017). Non–Small Cell Lung Cancer, Version 5.2017, NCCN Clinical Practice Guidelines in Oncology. Journal of the National Comprehensive Cancer Network. 15 (4): 504–535.

[7] C. Ho, K. Ramsden, Y. Zhai, N. Murray, S. Sun, B. Melosky, J. Laskin. (2014). Less Toxic Chemotherapy Improves Uptake of All Lines of Chemotherapy in Advanced Non–Small-Cell Lung Cancer: A 10-Year Retrospective Population-Based Review. Journal of Thoracic Oncology. 9 (8): 1180–1186.

[8] R. L. Siegel, K. D. Miller, A. Jemal. (2018). Cancer statistics, 2018. CA: A Cancer Journal for Clinicians. 68 (1): 7–30.

[9] Assessment, U. E. N. C. for E. (2009, March 15). SEER cancer statistics review, 1975-2012 [WEB SITE].

[10] M. Reck, D. F. Heigener, T. Mok, J. C. Soria, K. F. Rabe. (2013). Management of non-small-cell lung cancer: Recent developments. Lancet (London, England). 382 (9893): 709–719.

[11] D. D. Bahali. (2006). Habitat of Iridaceae in India. Bulletin of the National Institute of Ecology. 17 (1).

[12] S. K. Patnaik, S. Ayyamperumal, D. Jade, N. Palathoti, K. S. Akey, S. Jupudi, M. A. Harrison, S. Ponnambalam, N. Mj, C. Mjn. (2023). Virtual high throughput screening of natural peptides against ErbB1 and ErbB2 to identify potential inhibitors for cancer chemotherapy. Journal of Biomolecular Structure & Dynamics. 1–24.

[13] A. K. Swaroop, P. K. K. Namboori, M. Esakkimuthukumar, T. K. Praveen, P. Nagarjuna, S. K. Patnaik, J. Selvaraj. (2023). Leveraging decagonal in-silico strategies for uncovering IL-6 inhibitors with precision. Computers in Biology and Medicine. 163: 107231.

[14] A. K. Swaroop, S. K. Patnaik, J. Mr, P. K. Mr. (2022). Design and synthesis of novel quercetin metal complexes as IL-6 inhibitors for anti-inflammatory effect in SARS-CoV-2. Indian Journal of Biochemistry and Biophysics. 59 (8).